J. Dairy Sci. 109:6024–6034
https://doi.org/10.3168/jds.2025-27572

Functional interactions of Gp22 and Gp23 with Gp21 DNA helicase define the replication module of dairy-relevant *Ceduovirus* phage 94p4

Anna Santo,[1] Magdalena Chmielewska-Jeznach,[1,2] Tamara Aleksandrzak-Piekarczyk,[1] and Agnieszka K. Szczepankowska[1]*
[1]Institute of Biochemistry and Biophysics, Polish Academy of Sciences, 02-106 Warsaw, Poland
[2]Medical University of Warsaw, Department of Medical Biology, 00-575 Warsaw, Poland

ABSTRACT

Lactococcus lactis and *Lactococcus cremoris* strains play a vital role in dairy fermentations, yet their industrial use is threatened by bacteriophage infections that can lead to production failures. Replicative helicases are motor proteins driving genome replication, and their activity is often supported by accessory proteins involved in helicase recruitment, loading onto DNA, and regulation. However, in most phages of gram-positive bacteria, such factors remain largely uncharacterized. Here, we identify and functionally characterize 2 proteins, Gp22 and Gp23, encoded by genes located immediately downstream of the helicase gene *gp21* in the lytic *Ceduovirus* phage 94p4 infecting *L. lactis* and *L. cremoris* strains. Our findings demonstrate that Gp22 is a DNA-binding protein, lacking inherent helicase activity, which attenuates the DNA unwinding function of Gp21. In contrast, Gp23 lacks both DNA-binding and intrinsic unwinding activity, but significantly enhances DNA unwinding by Gp21. Protein interaction assays confirmed that both Gp22 and Gp23 bind directly to Gp21, suggesting they function as helicase-associated accessory proteins. This study provides the first functional insight into 2 phage-encoded proteins that modulate the Gp21 helicase and may regulate DNA processing during phage replication. These findings advance our understanding of the molecular mechanisms behind phage propagation in *Lactococcus* spp., bacteria that are integral to starter cultures used in the dairy industry worldwide. By characterizing replication-related phage proteins, this work contributes to expanding the knowledge on phage biology with potential relevance for the development of phage control strategies in the dairy industry.

Key words: *Lactococcus*, bacteriophage, dairy fermentation, phage replication, helicase-accessory proteins

INTRODUCTION

Replicative helicases are ubiquitous ring-shaped motor proteins that couple the hydrolysis of nucleoside triphosphates with the separation of duplex nucleic acids. Efficient helicase function allows successful phage genome replication, contributing also in recombination and repair. This is particularly relevant for bacteriophages infecting *Lactococcus lactis* and *Lactococcus cremoris*, key starter bacteria in dairy fermentations, where phage attacks can lead to acidification delays and serious fermentation failures. Despite their industrial significance, the replication mechanisms of lactococcal phages remain poorly understood.

Proper helicase activity during DNA replication requires coordination with a variety of partner proteins, including single-stranded DNA-binding proteins (**SSB**), primases, clamp-loader complexes, DNA polymerases, topoisomerases, and helicase loaders. The SSB prevent re-annealing of separated strands and stabilize intermediates before helicase loading (Xu et al., 2023). Helicase loaders directly recruit helicases to DNA (Davey and O'Donnell, 2003; Li and Araki, 2013), whereas clamp loaders assist helicase assembly at replication forks (Afonso et al., 2013). Topoisomerases, such as topo IV, alleviate supercoiling generated by helicase progression (Vos et al., 2011), and interactions with primases or DNA polymerases enhance helicase processivity (Makowska-Grzyska and Kaguni, 2010; Patel et al., 2011).

The strategies of helicase recruitment, loading, and activation differ widely across organisms and rely on distinct protein sets. These mechanisms are best characterized in the gram-negative model *Escherichia coli*, where the AAA+ ATPase DnaC acts as helicase loader. DnaC forms a complex with the replicative helicase DnaB and delivers it to the origin of replication (*ori*) (Arias-Palomo

Received September 9, 2025.
Accepted February 14, 2026.
*Corresponding author: agaszczep@ibb.waw.pl

The list of standard abbreviations for JDS is available at adsa.org/jds-abbreviations-26. Nonstandard abbreviations are available in the Notes.

et al., 2013). ATP hydrolysis triggers DnaC dissociation and activates DnaB-mediated unwinding. This process is further supported by interaction with the initiator protein DnaA (Kaguni, 2014). At collapsed forks, recruitment of DnaB is assisted by the primosome proteins PriA, PriB, PriC, and DnaT (Marians, 2000).

In gram-positive model bacterium *Bacillus subtilis*, the replicative helicase DnaC requires a dual helicase-loading system involving DnaI, DnaB, and DnaD (Velten et al., 2003; Núñez-Ramírez et al., 2007). DnaI, an AAA+ ATPase homologous to *E. coli* DnaC, assists in assembling the *B. subtilis* DnaC helicase. DnaB further promotes loading of the DnaC/DnaI complex, whereas DnaD stabilizes the interaction with the DnaA initiator and single-stranded DNA (**ssDNA**; Bruand et al., 2005). Both DnaB and DnaD are DNA-binding accessory proteins containing 2 distinct oligomerization domains (DDBH1/2) that mediate tetramerization and higher order ssDNA-dependent assemblies (Marston et al., 2010). Many bacteria, however, lack DnaC or DnaI homologs and employ alternative loading strategies, often using non-AAA+ proteins termed helicase operators (Blaine et al., 2023). Examples include DciA, which is widespread among bacterial phyla, particularly *Actinobacteria* and *Proteobacteria* (Brézellec et al., 2016), and domesticated phage-derived proteins DopE and DopC, described in some *Gammaproteobacteria* (Brézellec et al., 2017).

Bacteriophages likewise exhibit diverse strategies. Some encode complete replication modules, whereas others rely in part on host proteins. For instance, phage T4 uses Gp59 to recruit Gp41 helicase (Jones et al., 2001; Ishmael et al., 2002), and *B. subtilis* phage SPP1 employs G39P to load G40P helicase at *ori* via G38P (Ayora et al., 1999). In other viruses, helicase enzymes are fused with additional enzymatic domains, such as T7 Gp4 primase-helicase or SV40 LTag initiator-helicase, allowing autonomous recruitment and DNA loading (Ahnert et al., 2000; Chang et al., 2013). In lytic *Lactococcus* spp. phages, replication proteins have largely remained experimentally unvalidated, with the notable exception of recent studies characterizing ATP-dependent DNA helicases of *Skunavirus* and *Ceduovirus* phages (Chmielewska-Jeznach et al., 2022; Santo et al., 2025).

Considering the substantial influence of lactococcal phages on dairy fermentations, uncovering their replication mechanisms is essential for understanding phage biology in industrially relevant microbial systems. Our work investigates the activity of the Gp21 helicase from *Ceduovirus* phage 94p4, a phage previously isolated from a dairy environment (Chmielewska-Jeznach et al., 2020), in interaction with 2 previously uncharacterized proteins, Gp22 and Gp23, encoded in its direct genomic vicinity. Although these proteins lack homology to known protein families, our functional analyses suggest that Gp22 may act as a DNA-binding scaffold or loader mimic, whereas Gp23 functions as an activating cofactor that promotes helicase activity. Through combined DNA binding, unwinding, and protein-protein interaction assays, we demonstrate their roles as phage-specific helicase modulators.

MATERIALS AND METHODS

Bacteriophages, Bacterial Strains, and Growth Conditions

Bacterial strains are listed in Supplemental Table S1 (see Notes). *Escherichia coli* strains were grown at 37°C with shaking in Luria-Bertani (**LB**) broth or on LB agar plates (1.5% agar, wt/vol) or MacConkey agar supplemented with 1% maltose (MacConkey-maltose). When required, plates were supplemented with ampicillin (**Amp**; 100 µg/mL), kanamycin (**Kan**; 50 µg/mL), or isopropyl β-D-1-thiogalactopyranoside (**IPTG**; 0.15 m*M*). *Lactococcus cremoris* MG1363 was grown at 30°C without shaking in M17 broth supplemented with 0.5% glucose (GM17) or on GM17-agar plates. Bacteriophage 94p4 (vB_Llc_bIBB94p4; GenBank accession no. MH779521) isolated previously from the dairy environment was propagated in GM17 broth supplemented with 10 m*M* $CaCl_2$ using *L. cremoris* MG1363 as the host, as described previously (Chmielewska-Jeznach et al., 2020).

Cloning of gp22 and gp23

Cloning of *gp22* and *gp23* was carried out essentially as described for *gp21* (Santo et al., 2025). Open reading frames were amplified by PCR from phage 94p4 lysate using gp22_for/gp22_rev and gp23_for/gp23_rev primers, respectively (Supplemental Table S2, see Notes). Amplicons were cloned into the *Sap*I and *Pst*I restriction sites (Thermo Fisher Scientific, Waltham, MA) of the pTYB21 expression vector (New England BioLabs, Ipswich, MA). Recombinant plasmids were introduced into *E. coli* ER2566 cells by electroporation (Green and Sambrook, 2020). Selection was performed on LB agar containing Amp and verified by colony PCR using primers pTYB21_F and pTYB21_R and by sequencing.

Protein Overproduction and Purification

Overexpression of *gp21*, *gp22*, and *gp23* and subsequent protein purification were carried out with the IMPACT Kit (New England BioLabs; #E6901S) according to the manufacturer's instructions. The proteins were produced as N-terminal fusions to intein-chitin-binding domain (**CBD**) tags from pTYB21-derived plasmids (Supplemental Table S3, see Notes) as described previously (Santo et al., 2025). Briefly, *E. coli* ER2566 car-

rying pTYB21:*gp21*, pTYB21:*gp22* or pTYB21:*gp23* were grown in 1 L of LB broth supplemented with Amp at 28°C with shaking to an optical density at 600 nm of ~0.7. Cultures were induced with IPTG (0.4 m*M*, final concentration) to initiate recombinant protein production and incubated overnight at 15°C with shaking. Cell pellets were harvested and resuspended in 30 mL of chitin column buffer (50 m*M* Tris-HCl, pH 8.0, 500 m*M* NaCl, 10 m*M* $MgCl_2$), followed by disruption by sonication on ice (amplitude 16, 5 min, 15-s on/off cycles). The clarified lysates were loaded onto the chitin resin column and rinsed with 200 mL of chitin column buffer. Target proteins were released from the intein—CBD tag by on-column cleavage with 50 m*M* dithiothreitol (**DTT**) in the same buffer during 40-h incubation at 23°C.

Further purification was carried out by ion exchange chromatography on the ÄKTA Purifier (GE Healthcare, Chicago, IL) using HiTrap columns (Cytiva, Marlborough, MA) selected according to protein properties: Q XL for Gp21, SP HP for Gp22, and Heparin HP for Gp23. Columns were equilibrated with the calibration buffer (50 m*M* Tris-HCl, pH 8.0, 100 m*M* NaCl, 1 m*M* DTT). Proteins were eluted with a linear NaCl gradient (up to 1 *M* NaCl in the same buffer). Fractions were analyzed by SDS-PAGE and concentrated protein samples were stored in 50% (vol/vol) glycerol at −20°C. Protein concentrations were determined using the Bradford assay (Kielkopf et al., 2020).

Size Exclusion Chromatography

Size exclusion chromatography (**SEC**) of purified Gp21, Gp22, and Gp23 proteins was performed using the ÄKTA Purifier system (GE Healthcare, Chicago, IL) equipped with a Superdex 200 10/300 column (Sigma-Aldrich, St. Louis, MO). The column was equilibrated with gel filtration buffer (50 m*M* Tris-HCl pH 8.0, 300 m*M* NaCl) and calibrated with molecular mass standards (BioRad, Warsaw, Poland): thyroglobulin (670 kDa), γ-globulin (158 kDa), ovalbumin (44 kDa), myoglobin (17 kDa), and vitamin B_{12} (1.35 kDa). Protein samples (6.56 nmol) were loaded individually, eluted at 0.5 mL/min at room temperature, and fractions were analyzed by SDS-PAGE. Molecular weights of the eluted proteins were estimated from the standard calibration curve.

Electrophoretic Mobility-Shift Assay

DNA binding of Gp22 and Gp23 was tested with Cy5-labeled substrates: a 110-nt single-stranded oligonucleotide, a 110-bp double-stranded DNA (**dsDNA**) amplified by PCR using ori110_F and ori110_R primers and a forked substrate (30duplex5′) prepared as described by Curti et al. (2007) using dplx5′F/dplx5′R primers (Supplemental Table S2) with phage c2 lysate as template. Binding reactions (20 µL) contained 1.5 n*M* DNA substrate, the indicated protein, binding buffer (20 m*M* Tris-HCl, pH 8.0, 50 m*M* NaCl, 1 m*M* DTT, 1 m*M* EDTA, 2.5% glycerol), 0.1 mg/mL BSA, MilliQ water, and when indicated ATP (5 m*M*). Samples were incubated for 30 min at 30°C, resolved on 7% native polyacrylamide gels (0.5× Tris–borate–EDTA buffer [**TBE**], 100 V, 20–40 min), and visualized using a FluorChemQ MultiImageIII ChemiImager (Alpha Innotech, San Leandro, CA). DNA-protein complexes were quantified by densitometry using ImageJ (Image Processing and Analysis in Java, National Institutes of Health, Bethesda, MD). The DNA-only control lane was used as reference corresponding to 0% binding (free DNA band set to 100%). For DNA-protein samples, the intensity of the unbound DNA band was measured relative to the control, and the percentage of bound substrate was calculated by subtracting the relative amount of unbound DNA from the reference. Binding data were plotted against protein concentration and fitted to a "specific binding with Hill slope" model in GraphPad Prism (GraphPad Software, San Diego, CA) to derive dissociation constants (K_d) and Hill coefficients (h; Supplemental File S1, see Notes). All experiments were performed in 3 independent replicates, unless indicated otherwise.

Helicase Activity Assay

Helicase activity was examined in standard reaction mixtures (20 µL) containing the indicated protein(s), reaction buffer (50 m*M* Tris-HCl pH 8.0, 5 m*M* $MgCl_2$, 50 m*M* NaCl), 5 m*M* ATP, and 1.5 n*M* Cy5-labeled DNA substrate, with MilliQ water added to volume (Santo et al., 2025). Reactions were incubated at 30°C for 30 min and stopped by adding 6 µL of stop buffer (10% glycerol, 0.4% SDS, 50 m*M* EDTA). For reactions containing Gp22, 5 µL of proteinase K (20 mg/mL) was added (where indicated) together with the stop buffer, followed by incubation for 15 min at 37°C to release DNA from nucleoprotein complexes. Samples were resolved on pre-run 15% polyacrylamide gels (0.5× TBE, 100 V, 20–40 min) and visualized using a FluorChemQ MultiImageIII ChemiImager (Alpha Innotech, San Leandro, CA). Helicase activity was quantified by ImageJ. For each reaction lane, the total DNA signal was calculated as the sum of duplex (intact) and unwound DNA band intensities, and the fraction of unwound DNA was determined as the ratio of unwound DNA to total DNA signal, expressed as a percentage. The DNA unwinding activity was plotted against protein concentration and fitted using a 3-parameter nonlinear regression model (agonist vs. response) in GraphPad Prism to determine apparent protein concentration required for half maximal DNA unwinding

(EC_{50}) values (Supplemental File S2, see Notes). All experiments were performed in 3 independent replicates.

BACTH Assay

The bacterial adenylate cyclase 2-hybrid (**BACTH**) assay was carried out essentially as described by Karimova et al. (1998). The *gp21*, *gp22*, and *gp23* genes were PCR-amplified from the phage 94p4 lysate using specific primers (Supplemental Table S2) and cloned into BACTH vectors (Supplemental Table S3) via the restriction sites listed in Supplemental Table S2, generating in-frame fusions with either the T18 or T25 fragments of adenylate cyclase. Recombinant plasmids were introduced into *E. coli* DH5α for propagation and verified by sequencing. For interaction analysis, plasmids were introduced in pairs into *E. coli* BTH101 and plated on MacConkey agar containing 1% maltose, Amp, Kan, and IPTG. Colonies were examined for red coloration after 48-h incubation at 30°C. For quantitative assays, overnight cultures of cells harboring both plasmids were grown in LB medium with Amp, Kan, and IPTG, and β-galactosidase activity was determined according to Miller (1972). Empty vectors pKNT25M and pUT18CM served as negative controls (Supplemental File S3, see Notes).

Bioinformatic Analysis

The AA sequences of Gp22 and Gp23 proteins were analyzed using bioinformatics on-line tools at default settings such as BLASTp to compare the protein sequences against the nonredundant protein sequence database (Altschul et al., 1990) or HHpred to predict the secondary and tertiary structures of the proteins by comparing them against the Protein Data Bank database (Zimmermann et al., 2018). Schematic representation and comparison of the genomic regions (in GenBank format) were made using the Easyfig v2.2.5 software (at minimal length: 50 bp, maximal e-value: 0.1, minimal identity value: 20; Sullivan et al., 2011).

RESULTS

Computational Analysis of gp22 and gp23

In the *Ceduovirus* phage 94p4 genome, the *gp22* and *gp23* genes are located directly downstream of *gp21*, which encodes a DNA helicase (Santo et al., 2025). BlastP analysis showed that *gp22* and *gp23* gene products share high sequence identity with proteins E6 (98%) and E7 (93%) of the prolate-headed *L. lactis* phage c2, both previously annotated as DNA polymerase subunits (Lubbers et al., 1995). Gp23 homologs are commonly distributed among ceduoviruses, majority of which were isolated from dairy plants, whereas Gp22 is found in only ~40% of sequenced members of this group (27 of 70 available as of July 2025). In genomes lacking *gp22*, its position is either replaced by a nonhomologous gene or absent altogether (Figure 1). Despite their partial conservation, neither Gp22 nor Gp23 has been functionally characterized. Searches against the Conserved Domain Database (https://www.ncbi.nlm.nih.gov/Structure/cdd/cdd.shtml), UniProt, and HHpred failed to reveal substantial homology to proteins with established roles in DNA replication. The genomic proximity of *gp22* and *gp23* to the helicase gene *gp21* suggests that these proteins may cooperate in initiating phage replication. Previous transcriptional analysis of phage c2 identified a promoter between *e5*, encoding a Gp21 homolog (98% identity), and *e6* with typical −35 and −10 consensus sequences recognized by the *L. lactis* housekeeping σ^{70}-family sigma factor RpoD (Araya et al., 1993; Lubbers et al., 1998). An identical sequence occurs between *gp21* and *gp22-gp23*, indicating that these genes may be transcribed separately from *gp21*.

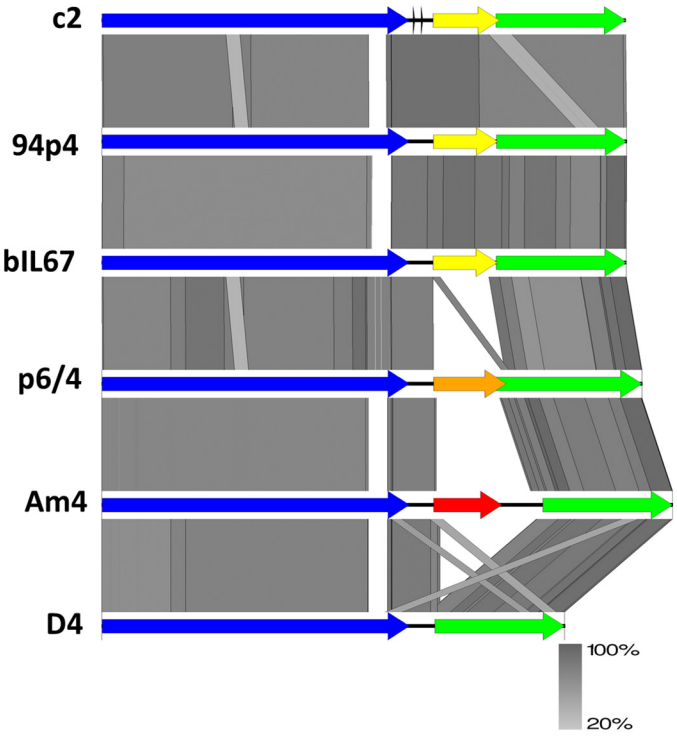

Figure 1. Comparative genomic alignment of the *gp21–gp23* region in representative *Ceduovirus* genomes. Genomic regions from selected phages closely related to 94p4 were compared using tBLASTx. Shaded areas between genomes represent regions of sequence similarity, with gradient shading reflecting percent identity (20%–100%). Predicted genes are shown as arrows: *gp21* (blue), *gp22* (yellow), *gp23* (green), or alternative nonhomologous genes occupying the *gp22* position (orange, red). Promoter sequences identified in phage c2 are marked as black arrows (−35 and −10 motifs).

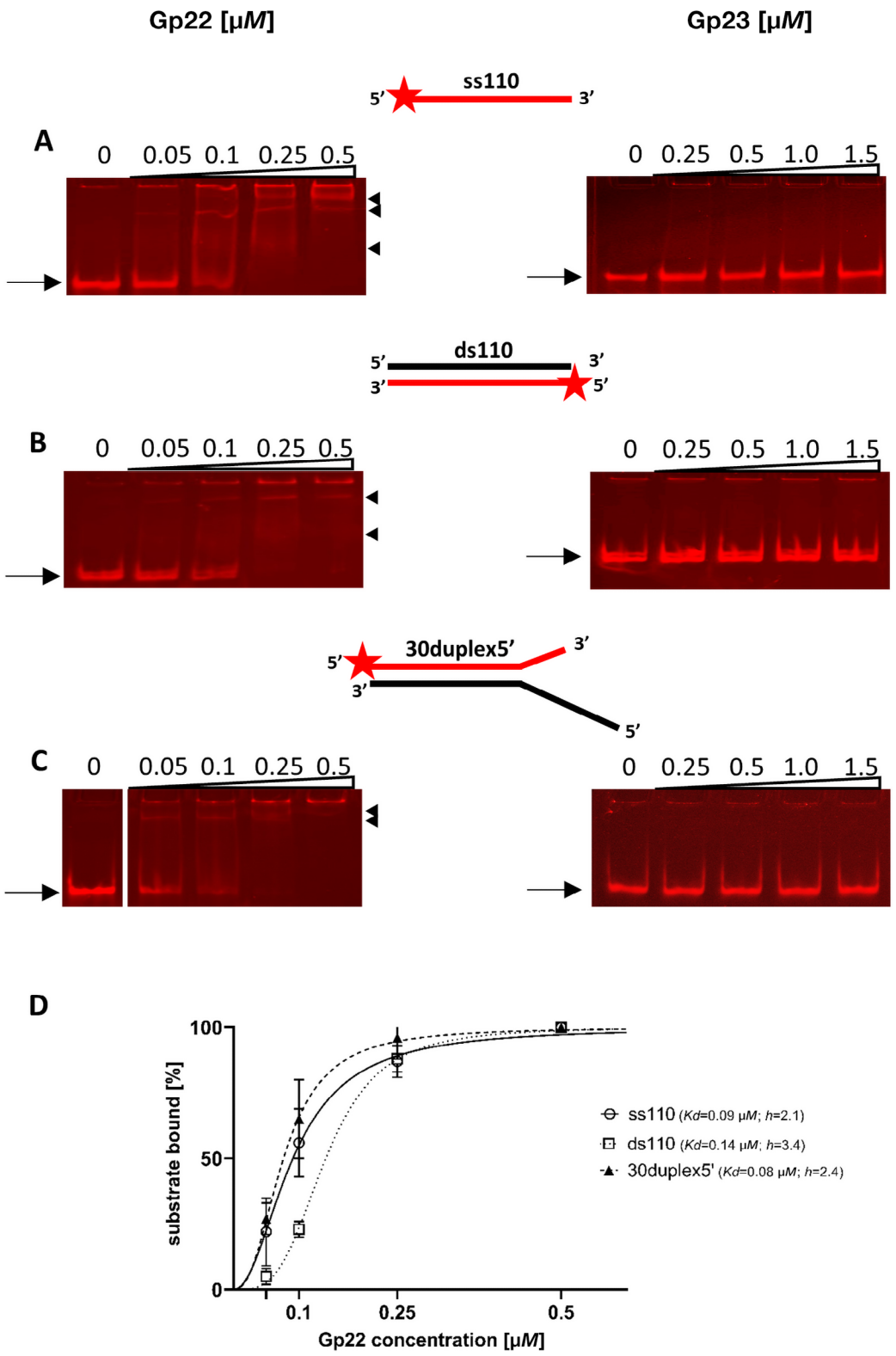

Figure 2. DNA-binding activity of Gp22 and Gp23. Increasing concentrations of proteins Gp22 (left panels) and Gp23 (right panels) were incubated with 1.5 n*M* Cy5-labeled (A) 110-nt single-stranded DNA (ss110), (B) 110-bp duplex DNA (ds110), or (C) branched duplex DNA substrate (30duplex5′). Nucleoprotein complexes with reduced electrophoretic mobility are marked by arrowheads; and free DNA is indicated by arrows. Cy5 labeling is denoted by a red star. (D) Quantitative analysis of Gp22 binding affinities to the tested substrates. Values represent means of 3 independent experiments; error bars indicate SD.

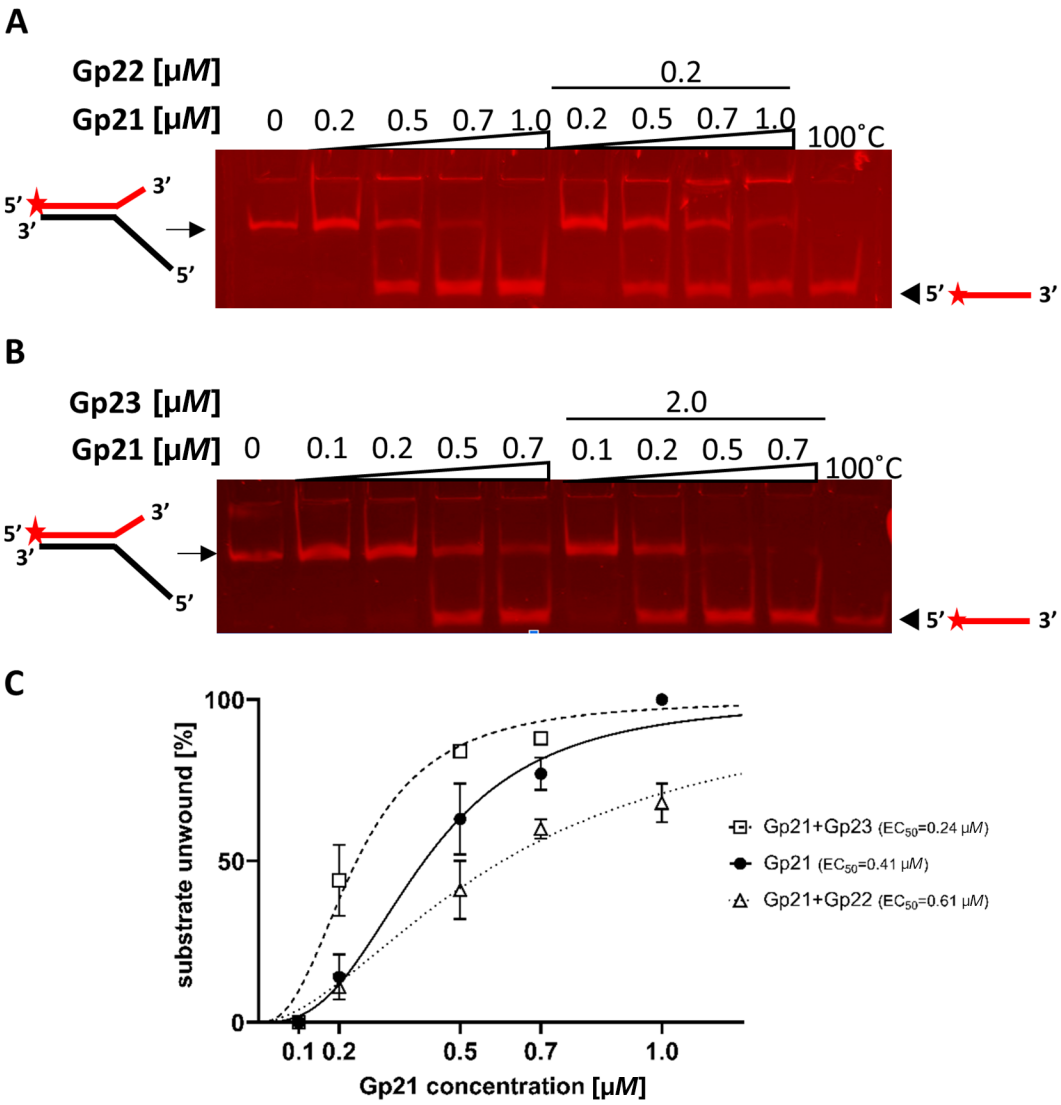

Figure 3. DNA unwinding activity of Gp21 in the presence of Gp22 and Gp23 proteins. The Cy5-labeled 30duplex5′ DNA substrate (1.5 n*M*) was incubated with increasing concentrations of Gp21 in the presence of (A) Gp22 (0.2 μ*M*) or (B) Gp23 (2 μ*M*). The expected position of the displaced Cy5-labeled strand is indicated by arrowheads, based on the migration of the heat-denatured substrate (100°C; control); arrows denote intact substrate. Cy5 labeling is denoted by a red star. (C) Quantitative analysis of Gp21 helicase activity in the presence or absence of Gp22 and Gp23. Data represent averages from at least 3 independent experiments; error bars indicate SD.

DNA-Binding Activity of Gp22 and Gp23

To examine the DNA-binding ability of purified Gp22 and Gp23 (Supplemental Figure S1, see Notes), electrophoretic mobility-shift assays (**EMSA**) with Cy5-labeled DNA substrates were performed (Figure 2). Gp22 bound efficiently to ssDNA (K_d = 0.09 μ*M*; Figure 2A, D) and to blunt-ended dsDNA (K_d = 0.14 μ*M*; Figure 2B, D), showing the highest affinity for duplex DNA carrying a free ssDNA overhang (K_d = 0.08 μ*M*; Figure 2C, D). Binding was strongly cooperative in all cases, with Hill coefficients (h) >2, and complete mobility shifts evident at 0.5 μ*M* Gp22 (Figure 2D). In contrast, Gp23 did not bind detectably to any tested substrate, even at the highest concentration applied (Figure 2). The ATP addition had no effect on the DNA-binding affinity of either protein (Supplemental Figure S2, see Notes). These results demonstrate that Gp22 recognizes a broad range of DNA structures, but Gp23 does not stably associate with DNA under the tested conditions.

Effect of Gp22 and Gp23 on the Gp21 Helicase Activity

To determine whether the helicase activity of Gp21 is influenced by Gp22 or Gp23, unwinding assays were

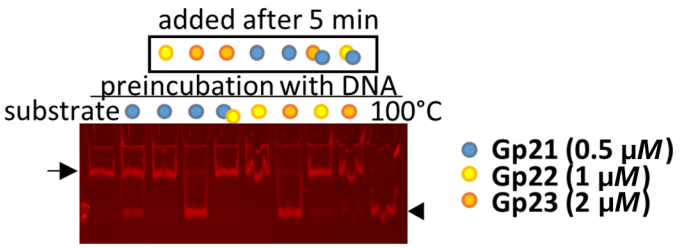

Figure 4. DNA unwinding assays testing the combined effects of Gp22 and Gp23 on Gp21 activity. The Cy5-labeled 30duplex5′ DNA substrate (1.5 n*M*) was preincubated for 5 min at 30°C with Gp21 (0.5 μ*M*), Gp22 (1 μ*M*), Gp23 (2 μ*M*), or combinations thereof, as indicated by colored dots above the lanes. Reactions were initiated by addition of the remaining proteins (black rectangle) and ATP. The expected position of the displaced Cy5-labeled strand is indicated by an arrowhead, based on the migration of the heat-denatured substrate (100°C control); arrow denotes the intact substrate.

performed using protein mixtures and the branched DNA substrate 30duplex5′ as a replication fork mimic. Gp21 alone exhibited robust helicase activity, effectively unwinding the substrate at concentration ≥0.7 μ*M* (Figure 3), consistent with our previous observations (Santo et al., 2025). Neither Gp22 nor Gp23 displayed unwinding activity on their own, even at elevated concentrations (Supplemental Figure S3, see Notes). At 0.1 μ*M* and above, Gp22 caused reduced substrate migration, consistent with formation of stable nucleoprotein complexes that require proteinase K for resolution (Supplemental Figure S3A). When combined with Gp21, Gp22 decreased helicase efficiency, shifting the EC_{50} from 0.41 μ*M* (Gp21 alone) to 0.61 μ*M* (Figure 3A, C). In contrast, the presence of Gp23 enhanced Gp21 activity, reducing the EC_{50} to 0.24 μ*M* (Figure 3B, C). Thus, Gp22 diminished and Gp23 promoted Gp21-mediated DNA unwinding under the tested conditions.

The influence of Gp22 and Gp23 on Gp21 helicase activity was also examined under different assembly assays that included a DNA preincubation step before addition of the remaining components and ATP (Figure 4). Gp22 suppressed Gp21 helicase activity under all tested conditions and irrespective of Gp23 presence, indicating that Gp22 strongly associates with DNA and prevents productive loading or progression of the helicase. In contrast, Gp23 alone enhanced DNA unwinding, regardless whether Gp21 was pre-incubated with DNA or added later.

Interaction of Gp21 with Gp22 and Gp23

Protein-protein interactions between Gp21 and either Gp22 or Gp23 were assessed in vivo using the BACTH assay. Among the tested combinations, strong interaction signals were observed between the N-terminal domains of Gp21 and Gp23, and between the C-terminus of Gp21 with the N-terminus of Gp22, as indicated by elevated β-galactosidase activity and red colony coloration (Figure 5). All other pairs displayed activity comparable to the negative control, indicating little or no interaction.

Gp21 Forms a Stable Complex with Gp23 but Not with Gp22

In vitro SEC analysis was used to examine whether Gp22 and Gp23 associate with Gp21. Individually, Gp22 and Gp23 eluted as peaks corresponding to a monomer (~8 kDa) and a dimer (~15 kDa), respectively (Supplemental Figure S4, see Notes), whereas Gp21 eluted at volumes consistent with its known hexameric state (Santo et al., 2025).

When all 3 proteins were mixed, the chromatogram revealed several peaks (Figure 6A). One of these contained both Gp21 and Gp23, as confirmed by SDS-PAGE (Figure 6B), demonstrating stable complex formation between the 2 proteins. In contrast, no stable Gp21-Gp22 complexes were detected, suggesting that either their interactions are transient or that they are destabilized under the tested conditions.

DISCUSSION

Replicative helicases do not act alone, but rely on accessory proteins that modulate their recruitment, loading onto DNA, and activity. Although accessory proteins for helicases of phages infecting gram-negative bacteria (e.g., T4 Gp59, λ P protein) are well-characterized, analogous proteins in most gram-positive bacterial phages remain underexplored (Ishmael et al., 2002; Hayes et al., 2013). Among the few defined examples is G39P of *B. subtilis* phage SPP1, which guides the helicase G40P to the origin of replication (*ori*L) via the replisome organizer G38P (Ayora et al., 1999). In *L. lactis* phages, bioinformatic predictions identified putative replication proteins in temperate P335-type phages, but experimental work has largely focused on replisome organizers rather than helicase partners (Zúñiga et al., 2002; Weigel and Seitz, 2006).

Here, we provide direct functional evidence that 2 phage-encoded proteins, Gp22 and Gp23, modulate the activity of the *Ceduovirus* helicase Gp21 from dairy phage 94p4 (Santo et al., 2025). Gp22 binds a range of DNA substrates with high affinity but does not unwind DNA on its own and consistently decreases Gp21-mediated unwinding. In contrast, Gp23 shows no detectable DNA binding yet enhances Gp21 helicase activity, particularly at lower helicase concentrations. The BACTH analyses indicate that both Gp22 and Gp23 interact with Gp21 and SEC assays further demonstrate that Gp21 and Gp23 form a stable complex in solution, although

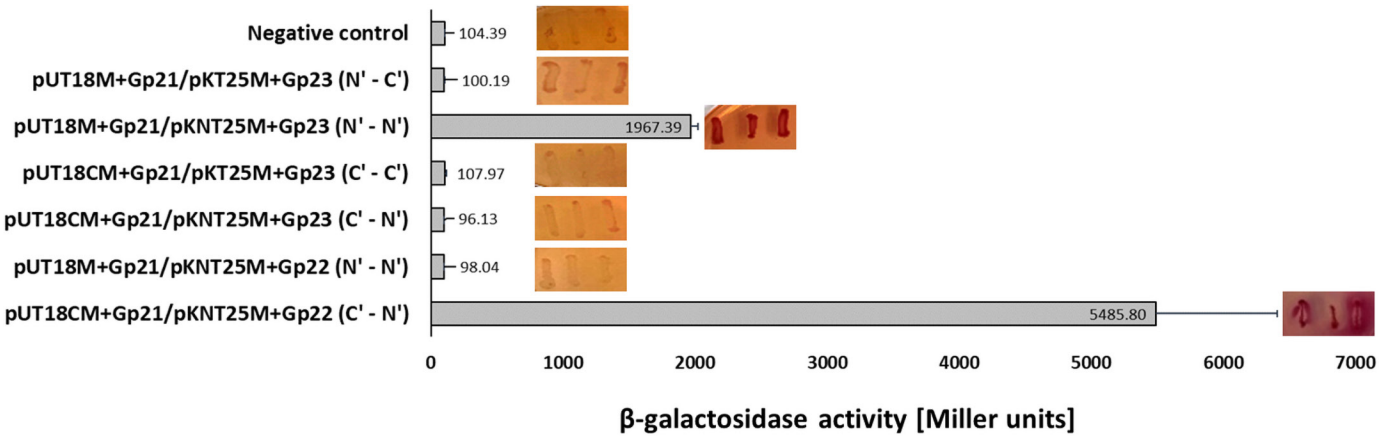

Figure 5. Interaction of Gp21 with Gp22 and Gp23 in the BACTH assay. *Escherichia coli* BTH101 carrying fusions of the tested proteins to the T18 and T25 fragments of adenylate cyclase were assayed. Interactions were detected by β-galactosidase activity (Miller units) and red colony coloration on MacConkey-maltose plates. Free terminal ends of the tested proteins are denoted as N′ and C′, respectively. Negative controls included cells harboring empty BACTH vectors. Data represent the mean of 3 technical replicates from 3 independent experiments; error bars indicate SD.

no stable Gp21–Gp22 interaction is detected under the same conditions. As BACTH is performed in living bacterial cells, it supports the notion that these contacts can form under cellular constraints (e.g., expression and folding). Nevertheless, as a heterologous system, it does not recapitulate the native infection context, including physiological stoichiometries, spatial organization, or competition with additional partners, and thus reflects interaction potential rather than interaction strength or dynamics in the native host. Complementary validation in the native or near-native context (e.g., co-immunoprecipitation, pull-down assays, or in vivo localization studies) would help establish the functional significance of these interfaces. Together, these findings support a model in which Gp23 acts as an activator of Gp21 before or during productive DNA engagement, whereas Gp22 functions as an inhibitory, DNA-sequestering factor that may limit helicase activity and prevent premature or excessive DNA unwinding. Further experiments will be needed to clarify the mechanistic basis of Gp22–Gp23–Gp21 interplay, including direct analysis of complex formation and binding order.

Although proteins with directly equivalent activities have not been described in other systems, conceptual parallels exist in which accessory proteins coordinate helicase activity with replication events. The behavior of Gp23 resembles bacterial helicase loaders (e.g., DnaC in *E. coli*, DnaI in *B. subtilis*), which assist helicase recruitment and activation yet do not remain part of the processive complex (Davey et al., 2002; Soultanas, 2002; Makowska-Grzyska and Kaguni, 2010). Unlike classical loaders, however, Gp23 lacks ATPase and DNA-binding activities, suggesting a loader-like but noncanonical role, potentially an allosteric activator that stabilizes a Gp21 conformation competent for productive oligomerization or DNA engagement. Dissecting the precise step at which Gp23 acts (ring closure, conformational activation, prevention of nonproductive assemblies) will require structural and kinetic studies (e.g., cryo-EM of Gp21 ± Gp23 or time-resolved unwinding assays). Gp22 diminishes Gp21-mediated unwinding and exhibits strong, ATP-independent DNA binding with EMSA indicating formation of stable nucleoprotein complexes. These features are consistent with a noncatalytic negative regulator that restricts helicase access or stabilizes DNA states unfavorable for translocation. Conceptually similar inhibitory or checkpoint functions have been described for proteins that regulate replication initiation, such as the archaeon *Sulfolobus solfataricus* Cdc6-1 and Cdc6-3, which bind DNA and interact with the cognate minichromosome maintenance (MCM) helicase, inhibiting its loading and DNA unwinding activities (De Felice et al., 2006; Jiang et al., 2007). Although our study did not examine the phage replication in vivo, the activities of Gp22 and Gp23 in the context of Gp21 function are consistent with roles in early-to-mid stages of the replication cycle. Proteins involved in helicase loading and activation are typically synthesized shortly after infection to initiate DNA replication. Given that the phage genome replication may involve multiple initiation events during a single infection cycle, Gp22 and Gp23-mediated regulation of Gp21 could plausibly act repeatedly, for example both during replication initiation and replication restart at stalled replication forks. The precise temporal engagement of these factors in vivo remains to be established.

The variable presence of *gp22* in *Ceduovirus* genomes suggests that this factor is not universally required and may be substituted by nonhomologous proteins, point-

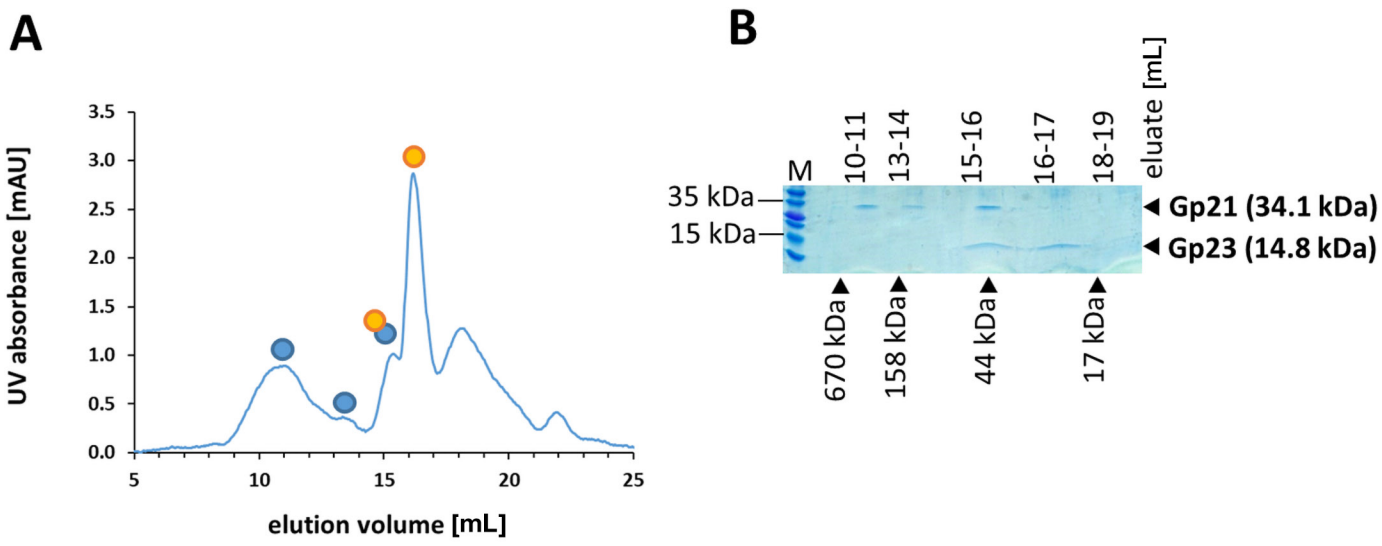

Figure 6. SEC analysis of Gp21 interactions with Gp22 and Gp23. (A) SEC elution profile of the Gp21, Gp22, and Gp23 mixture. Elution peaks in which Gp21 (blue dot) and Gp23 (orange dot) were detected are indicated. (B) SDS-PAGE of peak fractions showing co-elution of Gp21 with Gp23 but not with Gp22. Black triangles indicate molecular mass standards.

ing to a flexible replication module that can be tuned to phage or host context. This modularity aligns with the genomic organization of phage replication clusters (Hatfull and Hendrix, 2011) and with documented plasticity in lactic acid bacteriophages (Brüssow and Desiere, 2001). The arrangement of *gp21-gp22-gp23* adjacent but likely separately transcribed (by analogy to c2 *e5* vs. *e6–e7*; Lubbers et al., 1998) further suggests temporal regulation across replication stages. From an applied perspective relevant to dairy fermentations, diversity in replication modules may underlie differences in propagation kinetics among lactococcal phages. Phages encoding activator-like Gp23 but lacking antagonistic Gp22 could, in principle, replicate more rapidly and pose a higher risk of rapid starter culture lysis, whereas the presence of Gp22-like inhibitors may temper replication efficiency.

As phage infections targeting *Lactococcus* spp. starter strains are a major cause of fermentation failures and substantial economic losses, elucidation of the replication mechanisms of dairy phages and the interplay among replication proteins can support the design of preventative tools. Mechanistic insights into replication modules can translate into improved phage-control workflows in dairy plants. For example, replication-module genes such as *gp22* and *gp23* may serve as molecular markers for monitoring incoming phage populations and stratifying risk, guiding starter culture rotation or selection of phage-resistant strains. In parallel, knowledge of phage-host interactions could support the engineering or selection of strains with effective native defense systems (e.g., CRISPR-Cas or restriction-modification). In the longer term, structural and functional characterization of essential replication enzymes, such as helicases, could enable the development of selective inhibitors to reduce phage propagation during fermentation without compromising starter culture performance. Replication-module genes, such as *gp22* and *gp23*, therefore represent potential tools and targets for safeguarding dairy fermentation processes and improving starter culture robustness.

NOTES

ÄKTA Purifier system was sponsored in part by the Centre for Preclinical Research and Technology (CePT), a project co-sponsored by the European Regional Development Fund Innovate Economy, the National Cohesion Strategy of Poland. This study was partially financed by the Minigrant 2020 no. SBM/01-20 of the School of Molecular Biology, IBB PAS. Supplemental material for this article is available at https://doi.org/10.5281/zenodo.18504989. No human or animal subjects were used, so this analysis did not require approval by an Institutional Animal Care and Use Committee or Institutional Review Board. The authors have not stated any conflicts of interest.

Nonstandard abbreviations used: Amp = ampicillin; BACTH = bacterial adenylate cyclase 2-hybrid; CBD = chitin-binding domain; dsDNA = double-stranded DNA; DTT = dithiothreitol; EC_{50} = apparent protein concentration required for half maximal DNA unwinding; EMSA = electrophoretic mobility-shift assays; IPTG = isopropyl

β-D-1-thiogalactopyranoside; Kan = kanamycin; K_d = dissociation constants; LB = Luria-Bertani; SEC = size exclusion chromatography; SSB = single-stranded DNA-binding; ssDNA = single-stranded DNA; TBE = Tris–borate–EDTA buffer.

REFERENCES

Afonso, J. P., K. Chintakayala, C. Suwannachart, S. Sedelnikova, K. Giles, J. B. Hoyes, P. Soultanas, J. B. Rafferty, and N. J. Oldham. 2013. Insights into the structure and assembly of the *Bacillus subtilis* clamp-loader complex and its interaction with the replicative helicase. Nucleic Acids Res. 41:5115–5126. https://doi.org/10.1093/nar/gkt173.

Ahnert, P., K. M. Picha, and S. S. Patel. 2000. A ring-opening mechanism for DNA binding in the central channel of the T7 helicase-primase protein. EMBO J. 19:3418–3427. https://doi.org/10.1093/emboj/19.13.3418.

Altschul, S. F., W. Gish, W. Miller, E. W. Myers, and D. J. Lipman. 1990. Basic local alignment search tool. J. Mol. Biol. 215:403–410. https://doi.org/10.1016/S0022-2836(05)80360-2.

Araya, T., N. Ishibashi, S. Shimamura, K. Tanaka, and H. Takahashi. 1993. Genetic and molecular analysis of the *rpoD* gene from *Lactococcus lactis.* Biosci. Biotechnol. Biochem. 57:88–92. https://doi.org/10.1271/bbb.57.88.

Arias-Palomo, E., V. L. O'Shea, I. V. Hood, and J. M. Berger. 2013. The bacterial DnaC helicase loader is a DnaB ring breaker. Cell 153:438–448. https://doi.org/10.1016/j.cell.2013.03.006.

Ayora, S., A. Stasiak, and J. C. Alonso. 1999. The *Bacillus subtilis* bacteriophage SPP1 G39P delivers and activates the G40P DNA helicase upon interacting with the G38P-bound replication origin. J. Mol. Biol. 288:71–85. https://doi.org/10.1006/jmbi.1999.2662.

Blaine, H. C., L. A. Simmons, and C. L. Stallings. 2023. Diverse mechanisms of helicase loading during DNA replication initiation in bacteria. J. Bacteriol. 205:e0048722. https://doi.org/10.1128/jb.00487-22.

Brézellec, P., M.-A. Petit, S. Pasek, I. Vallet-Gely, C. Possoz, and J.-L. Ferat. 2017. Domestication of lambda phage genes into a putative third type of replicative helicase matchmaker. Genome Biol. Evol. 9:1561–1566. https://doi.org/10.1093/gbe/evx111.

Brézellec, P., I. Vallet-Gely, C. Possoz, S. Quevillon-Cheruel, and J.-L. Ferat. 2016. DciA is an ancestral replicative helicase operator essential for bacterial replication initiation. Nat. Commun. 7:13271. https://doi.org/10.1038/ncomms13271.

Bruand, C., M. Velten, S. McGovern, S. Marsin, C. Sérèna, S. D. Ehrlich, and P. Polard. 2005. Functional interplay between the *Bacillus subtilis* DnaD and DnaB proteins essential for initiation and re-initiation of DNA replication. Mol. Microbiol. 55:1138–1150. https://doi.org/10.1111/j.1365-2958.2004.04451.x.

Brüssow, H., and F. Desiere. 2001. Comparative phage genomics and the evolution of *Siphoviridae*: Insights from dairy phages. Mol. Microbiol. 39:213–223. https://doi.org/10.1046/j.1365-2958.2001.02228.x.

Chang, Y. P., M. Xu, A. C. Machado, X. J. Yu, R. Rohs, and X. S. Chen. 2013. Mechanism of origin DNA recognition and assembly of an initiator-helicase complex by SV40 large tumor antigen. Cell Rep. 3:1117–1127. https://doi.org/10.1016/j.celrep.2013.03.002.

Chmielewska-Jeznach, M., J. K. Bardowski, and A. K. Szczepankowska. 2020. *Lactococcus Ceduovirus* phages isolated from industrial dairy plants—From physiological to genomic analyses. Viruses 12:280. https://doi.org/10.3390/v12030280.

Chmielewska-Jeznach, M., K. Steczkiewicz, K. Kobyłecki, J. K. Bardowski, and A. K. Szczepankowska. 2022. An adenosine triphosphate-dependent 5′-3′ DNA helicase from sk1-like *Lactococcus lactis* F13 Phage. Front. Microbiol. 13:840219. https://doi.org/10.3389/fmicb.2022.840219.

Curti, E., S. J. Smerdon, and E. O. Davis. 2007. Characterization of the helicase activity and substrate specificity of *Mycobacterium tuberculosis* UvrD. J. Bacteriol. 189:1542–1555. https://doi.org/10.1128/JB.01421-06.

Davey, M. J., L. Fang, P. McInerney, R. E. Georgescu, and M. O'Donnell. 2002. The DnaC helicase loader is a dual ATP/ADP switch protein. EMBO J. 21:3148–3159. https://doi.org/10.1093/emboj/cdf308.

Davey, M. J., and M. O'Donnell. 2003. Replicative helicase loaders: Ring breakers and ring makers. Curr. Biol. 13:R594–R596. https://doi.org/10.1016/S0960-9822(03)00523-2.

De Felice, M., L. Esposito, M. Rossi, and F. M. Pisani. 2006. Biochemical characterization of two Cdc6/ORC1-like proteins from the crenarchaeon *Sulfolobus solfataricus.* Extremophiles 10:61–70. https://doi.org/10.1007/s00792-005-0473-0.

Green, M. R., and J. Sambrook. 2020. Transformation of *Escherichia coli* by electroporation. Cold Spring Harb. Protoc. 2020:101220. https://doi.org/10.1101/pdb.prot101220.

Hatfull, G. F., and R. W. Hendrix. 2011. Bacteriophages and their genomes. Curr. Opin. Virol. 1:298–303. https://doi.org/10.1016/j.coviro.2011.06.009.

Hayes, S., C. Erker, M. A. Horbay, K. Marciniuk, W. Wang, and C. Hayes. 2013. Phage lambda P protein: Trans-activation, inhibition phenotypes and their suppression. Viruses 5:619–653. https://doi.org/10.3390/v5020619.

Ishmael, F. T., S. C. Alley, and S. J. Benkovic. 2002. Assembly of the bacteriophage T4 helicase: Architecture and stoichiometry of the gp41-gp59 complex. J. Biol. Chem. 277:20555–20562. https://doi.org/10.1074/jbc.M111951200.

Jiang, P. X., J. Wang, Y. Feng, and Z. G. He. 2007. Divergent functions of multiple eukaryote-like Orc1/Cdc6 proteins on modulating the loading of the MCM helicase onto the origins of the hyperthermophilic archaeon *Sulfolobus solfataricus* P2. Biochem. Biophys. Res. Commun. 361:651–658. https://doi.org/10.1016/j.bbrc.2007.07.073.

Jones, C. E., T. C. Mueser, K. C. Dudas, K. N. Kreuzer, and N. G. Nossal. 2001. Bacteriophage T4 gene 41 helicase and gene 59 helicase-loading protein: A versatile couple with roles in replication and recombination. Proc. Natl. Acad. Sci. USA 98:8312–8318. https://doi.org/10.1073/pnas.121009398.

Kaguni, J. M. 2014. DnaA, DnaB, and DnaC. Pages 1–14 in Molecular Life Sciences. E. Bell, ed. Springer, New York, NY. https://doi.org/10.1007/978-1-4614-6436-5_142-1.

Karimova, G., J. Pidoux, A. Ullmann, and D. Ladant. 1998. A bacterial two-hybrid system based on a reconstituted signal transduction pathway. Proc. Natl. Acad. Sci. USA 95:5752–5756. https://doi.org/10.1073/pnas.95.10.5752.

Kielkopf, C. L., W. Bauer, and I. L. Urbatsch. 2020. Bradford assay for determining protein concentration. Cold Spring Harb. Protoc. 2020:102269. https://doi.org/10.1101/pdb.prot102269.

Li, Y., and H. Araki. 2013. Loading and activation of DNA replicative helicases: the key step of initiation of DNA replication. Genes Cells 18:266–277. https://doi.org/10.1111/gtc.12040.

Lubbers, M. W., K. Schofield, N. R. Waterfield, and K. M. Polzin. 1998. Transcription analysis of the prolate-headed lactococcal bacteriophage c2. J. Bacteriol. 180:4487–4496. https://doi.org/10.1128/JB.180.17.4487-4496.1998.

Lubbers, M. W., N. R. Waterfield, T. P. Beresford, R. W. Le Page, and A. W. Jarvis. 1995. Sequencing and analysis of the prolate-headed lactococcal bacteriophage c2 genome and identification of the structural genes. Appl. Environ. Microbiol. 61:4348–4356. https://doi.org/10.1128/aem.61.12.4348-4356.1995.

Makowska-Grzyska, M., and J. M. Kaguni. 2010. Primase directs the release of DnaC from DnaB. Mol. Cell 37:90–101. https://doi.org/10.1016/j.molcel.2009.12.031.

Marians, K. J. 2000. PriA-directed replication fork restart in *Escherichia coli.* Trends Biochem. Sci. 25:185–189. https://doi.org/10.1016/S0968-0004(00)01565-6.

Marston, F. Y., W. H. Grainger, W. K. Smits, N. H. Hopcroft, M. Green, A. M. Hounslow, A. D. Grossman, C. J. Craven, and P. Soultanas. 2010. When simple sequence comparison fails: The cryptic case of the shared domains of the bacterial replication initiation proteins DnaB and DnaD. Nucleic Acids Res. 38:6930–6942. https://doi.org/10.1093/nar/gkq465.

Miller, J. H. 1972. Experiments in molecular genetics. Cold Spring Harbor Laboratory, Cold Spring Harbor, NY.

Núñez-Ramírez, R., M. Velten, G. Rivas, P. Polard, J. M. Carazo, and L. E. Donate. 2007. Loading a ring: Structure of the *Bacillus subtilis* DnaB protein, a co-loader of the replicative helicase. J. Mol. Biol. 367:764–769. https://doi.org/10.1016/j.jmb.2006.12.075.

Patel, S. S., M. Pandey, and D. Nandakumar. 2011. Dynamic coupling between the motors of DNA replication: Hexameric helicase, DNA polymerase, and primase. Curr. Opin. Chem. Biol. 15:595–605. https://doi.org/10.1016/j.cbpa.2011.08.003.

Santo, A., M. Chmielewska-Jeznach, K. Steczkiewicz, T. Aleksandrzak-Piekarczyk, and A. K. Szczepankowska. 2025. Structural and functional insights into Gp21 as a new SF4 helicase of prolate-headed *Lactococcus lactis* phage 94p4. Int. J. Biol. Macromol. 320:145668. https://doi.org/10.1016/j.ijbiomac.2025.145668.

Soultanas, P. 2002. A functional interaction between the putative primosomal protein DnaI and the main replicative DNA helicase DnaB in *Bacillus.* Nucleic Acids Res. 30:966–974. https://doi.org/10.1093/nar/30.4.966.

Sullivan, M. J., N. K. Petty, and S. A. Beatson. 2011. Easyfig: A genome comparison visualiser. Bioinformatics 27:1009–1010. https://doi.org/10.1093/bioinformatics/btr039.

Velten, M., S. McGovern, S. Marsin, S. D. Ehrlich, P. Noirot, and P. Polard. 2003. A two-protein strategy for the functional loading of a cellular replicative DNA helicase. Mol. Cell 11:1009–1020. https://doi.org/10.1016/S1097-2765(03)00130-8.

Vos, S. M., E. M. Tretter, B. H. Schmidt, and J. M. Berger. 2011. All tangled up: how cells direct, manage and exploit topoisomerase function. Nat. Rev. Mol. Cell Biol. 12:827–841. https://doi.org/10.1038/nrm3228.

Weigel, C., and H. Seitz. 2006. Bacteriophage replication modules. FEMS Microbiol. Rev. 30:321–381. https://doi.org/10.1111/j.1574-6976.2006.00015.x.

Xu, L., M. T. J. Halma, and G. J. L. Wuite. 2023. Unravelling how single-stranded DNA binding protein coordinates DNA metabolism using single-molecule approaches. Int. J. Mol. Sci. 24:2806. https://doi.org/10.3390/ijms24032806.

Zimmermann, L., A. Stephens, S. Z. Nam, D. Rau, J. Kübler, M. Lozajic, F. Gabler, J. Söding, A. N. Lupas, and V. Alva. 2018. A completely reimplemented MPI bioinformatics toolkit with a new HHpred server at its core. J. Mol. Biol. 430:2237–2243. https://doi.org/10.1016/j.jmb.2017.12.007.

Zúñiga, M., B. Franke-Fayard, G. Venema, J. Kok, and A. Nauta. 2002. Characterization of the putative replisome organizer of the lactococcal bacteriophage r1t. J. Virol. 76:10234–10244. https://doi.org/10.1128/JVI.76.20.10234-10244.2002.

ORCIDS

Anna Santo, https://orcid.org/0000-0002-3144-7628
Magdalena Chmielewska-Jeznach, https://orcid.org/0000-0002-1976-8517
Tamara Aleksandrzak-Piekarczyk, https://orcid.org/0000-0002-4725-760X
Agnieszka K. Szczepankowska https://orcid.org/0000-0002-8733-3283